Persistent Homology based Classification of Chaotic Multi-variate Time Series with Application to EEG Data

Martina Flammer and Knut Hüper
Institute of Mathematics, Julius-Maximilians-Universität Würzburg, Emil-Fischer-Straße 31, Würzburg, Germany

Keywords: Bottleneck Distance, Dimension Reduction, Dynamical Component Analysis, Persistent Homology, Simplicial Complex, Topological Data Analysis.

Abstract: An application of persistent homology for detection of epileptic events in EEG data is presented. Given point cloud data, persistent homology is a tool from topological data analysis to describe the structure of the underlying space on which the data was sampled by utilizing topological invariants and tracking their behavior on several spatial scales. As a preprocessing step, a novel method called Dynamical Component Analysis is used that reduces the dimension of a multi-variate time series by incorporating information about the dynamics of the system. The results show that our proposed method is appropriate to detect the occurence of petit-mal epileptic seizures in EEG signals.

1 INTRODUCTION

According to the WHO, almost 50 million people suffer under epilepsy, which makes it one of the most frequent neurological diseases. Being unable to cure epilepsy, patients are usually dependent on medication, making the detection and forecast of epileptic events a particularly important task that is commonly accomplished by measuring brain activity using an electroencephalogram (EEG). These data are measured by placing electrodes on the scalp of patients that measure the summed electrical brain activity. However, even for experts it can be difficult and time-consuming to classify EEG data of every single patient, which makes the automated classification and interpretation of EEG data a tremendous challenge for data scientists from various fields, in particular, from a mathematical and an engineering point of view.

Since it is assumed that during epileptic events the activity of neurons is more synchronized, we believe that the EEG data set is revealing some mathematical structure that is the key ingredient to classify EEG data with respect to seizure and non-seizure activity. Such an assumption follows the paper (van Veen and Liley, 2006) where Shilnikov chaos was proposed during epileptic events.

Being on the intersection of topology, the traditional mathematical field that investigates structures, and data science, topological data analysis seems to be an appropriate approach to the above mentioned task. Especially its main method, persistent homology, is considered here as a procedure to describe the structure of spaces on which data was sampled. Basically, it uses tools from computational topology combined with geometric insight to provide connectivity information of the underlying space on several spatial scales. Having its theoretical fundaments in algebraic topology leads to a well-understood foundation of persistent homology. Further advantages are that the method is robust with respect to small perturbations of the input data and is able to cope with complex data sets, making it particularly useful for analysis of big data. Since the original formulation of persistent homology in the early 2000s, a lot of research is going on in order to extend the field in various directions and to complete the framework.

Although persistent homology is able to process high-dimensional data sets it still requires a lot of computational time. To circumvent this drawback we preprocess the data using Dynamical Component Analysis (DyCA) (Uhl et al., 2020), a novel method to reduce the dimension of a time series by regarding the dynamics of the underlying system. It can be applied whenever the dynamics is modeled by a system of ordinary differential equations (ODEs) with linear as well as non-linear equations, which is the case for EEG data (Friedrich and Uhl, 1996).

The outline of this paper is the following. In Section 2, the preprocessing of the data with DyCA is described. Section 3 will focus on the mathematical

Flammer, M. and Hüper, K.
Persistent Homology based Classification of Chaotic Multi-variate Time Series with Application to EEG Data.
DOI: 10.5220/0011144800003271
In *Proceedings of the 19th International Conference on Informatics in Control, Automation and Robotics (ICINCO 2022)*, pages 595-604
ISBN: 978-989-758-585-2; ISSN: 2184-2809

description of persistent homology, from its algebraic basics to its application to point cloud data and its visualization. In Section 4, the EEG data sets are specified that are used to test out proposed approach. Section 5 is devoted to the description of the exact procedure in our numerical experiments and the presentation of the results, which is followed by an outlook to future work in Section 6.

2 PREPROCESSING

In (Uhl et al., 2020), the authors introduced a novel method for dimensionality reduction and separating the deterministic part of the data from the stochastic part that corresponds to the noise components. This method, called DyCA, can be applied to multivariate time-series if the underlying model for the dynamics follows a system of ODEs which consists of linear as well as non-linear equations. Using the linear part, amplitudes and multivariate modes are determined that fit the system of ODEs optimally. This task is accomplished by solving a generalized eigenvalue problem that is derived from a least squares minimization problem. The eigenvalue problem leads to a collection of eigenvalues and associated eigenvectors together with some corresponding vectors v_i, which both together form the set of projection vectors. Eigenvalues close to 1 correspond to modes for which the linear approximation fits well. Introducing a threshold for the eigenvalues allows to estimate the number of linearly coupled components. Furthermore, also the total number of equations n, governed by the ODE system, is estimated as being the dimension of the span of the projection vectors. The set of eigenvectors u_i is completed by suitable v_i, where the v_i are the projection vectors corresponding to the non-linear equations, to a basis of $\mathbb{R}^n$, the relevant subspace. Using the projection vectors, one can project the initial multivariate time series onto the relevant subspace, which results in the estimated amplitudes.

The last step is again solving a least squares problem in order to obtain the pseudoinverse of the projection matrix and therefore get an estimate for the DyCA components. In the end, the time-varying signal is reconstructed as a linear combination of the estimated time-varying amplitudes and the estimated DyCA components. The derivation can be found in detail in the paper (Uhl et al., 2020).

The authors of (Uhl et al., 2020) thought of several ways to utilize DyCA, for example for using the eigenvalue spectrum to classify the dynamics of the time series, for eliminating noise components of the signal or for modeling the signal by an data-driven approach. In our paper, we use it as a preprocessing step for the projection of the given data onto a lower-dimensional subspace and for incidentally reducing the noise.

3 PERSISTENT HOMOLOGY

Persistent homology is a central topic in the field of topological data analysis. In topological data analysis, one frequently faces the problem that a set of data is given that was sampled on a space but the structure of the space is unknown. Persistent homology provides a tool which allows to study the topological invariants of this space by building a sequence of simplicial complexes from the data, also known as the persistence complex. By regarding several scales, which is accomplished by tracking the topology of the data set when the point cloud is thickened, one gets information about connectivity of the space, such as connected components, holes, voids, etc., which can be used for example for the analysis of networks, dynamical systems and protein structures. A detailed overview can be found in (Otter et al., 2017).

3.1 From Data to Simplicial Complexes

The first step in the pipeline of the computation of persistent homology consists of constructing a simplicial complex from the given point cloud data. A simplicial complex is a way to approximate a topological space by a set of vertices, edges, triangles, tetrahedrons and higher-dimensional equivalents. Such an approximation is called a triangulation of the space, however, not every space is triangulable, but in our application the assumption of triangulable spaces is appropriate.

Definition 3.1 (Simplicial complex)**.** A simplicial complex K is a set consisting of non-empty subsets of a set K_0 such that the following two properties hold:

1. $\{v\} \in K$ for all $v \in K_0$ and
2. $\tau \in K$ for all $\tau \subset \sigma, \sigma \in K$.

The elements of K are called *simplices* and elements of K_0 are referred to as *vertices of* K. A simplex is called *p-simplex* or equivalently, is said to have *dimension* p, if its cardinality is $p+1$. The *dimension* of the simplicial complex K is defined as the maximum of dimensions of all its simplices.

A simplex τ is called a *face* of a simplex σ if $\tau \subset \sigma$. τ is called a face of σ *of codimension* k if the dimensions of τ and σ differ by k. For two simplicial complexes K and L, a *map of simplicial complexes* $f : K \to L$ is a map on the corresponding vertex sets

$f : K_0 \to L_0$ with the property that simplices in K are mapped to simplices in L, i.e. $f(\sigma) \in L$ for all $\sigma \in K$.

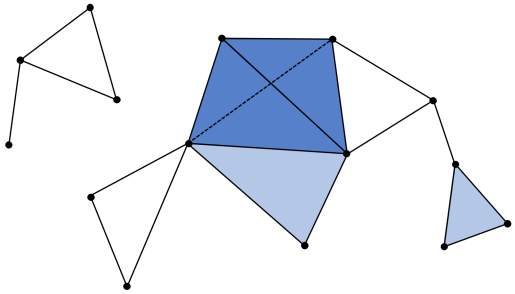

Figure 1: Example of a simplicial complex.

In Figure 1, an example of a three dimensional simplicial complex is shown. It consists of 0-simplices (points), of 1-simplices (edges between points), of 2-simplices (triangles) and of one 3-simplex (the tetrahedron).

Given data in form of a finite point cloud, there are several ways to construct a simplicial complex of that data set. One of the most important complexes is the so-called Čech complex.

Definition 3.2. For a finite point set M in a metric space X and some $\varepsilon > 0$, consider the non-empty union $M_\varepsilon = \bigcup_{x \in M} B(x, \varepsilon)$, where $B(x, \varepsilon)$ denotes the closed ball centered at x and with radius ε. Let $\check{C}(M, \varepsilon)$ be the simplicial complex with vertex set M and where a k-simplex $\{x_1, ..., x_k\} \subset M$ is added to the simplicial complex $\check{C}(M, \varepsilon)$ if and only if $B(x_1, \varepsilon) \cap \ldots \cap B(x_k, \varepsilon) \neq \emptyset$. $\check{C}(M, \varepsilon)$ is called the Čech complex on M at scale ε.

An example of a Čech complex at a certain scale ε is shown in Figure 2. The black dots denote the point cloud data set and the orange balls are the closed balls around each data point. As one can see in the Figure, an edge between two points is added to the simplicial complex if the intersection of the two associated balls is non-empty. In a analogue manner, triangles, tetrahedrons and higher-dimensional simplices are added.

Theoretically, the dimension of the Čech complex might become very large, namely up to $|M| - 1$. Additionally, in order to check whether a subset of M is actually a simplex, one has to check the above condition for a large number of intersections. This makes the calculation of the Čech complex computationally expensive. A way to overcome these difficulties is by regarding the *lazy* version of this simplicial complex. That means that one only checks for pairwise intersections, i.e. a simplex $\{x_1, ..., x_k\}$ is added to the simplicial complex if and only if the pairwise intersections $B(x_i, \varepsilon) \cap B(x_j, \varepsilon)$ are non-empty for all indices $1 \leq i < j \leq k$. We call this simplicial complex the

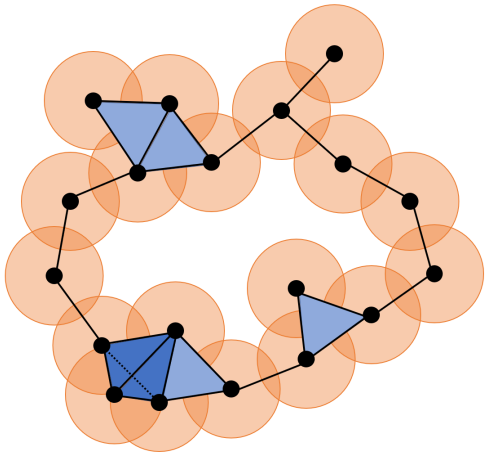

Figure 2: Example of a Čech complex.

Vietoris-Rips complex of M at scale ε. The Vietoris-Rips complex still can have a very large dimension, but it is computationally cheaper, making it one of the most popular choices for building a simplicial complex on point cloud data.

3.2 Simplicial Homology

Homology is a way of classifying topological spaces. The idea behind homology is to distinguish spaces by their n-dimensional holes, for every $n \in \mathbb{N}_0$. 0-dimensional holes correspond to connected components, 1-dimensional holes to holes in the usual sense, 2-dimensional holes to voids, and so on. The homology of a simplicial complex is constructed as follows:

Let $C_p(K)$ be the vector space over $\mathbb{F}_2$ with basis consisting of the p-simplices of K. Now, we define linear maps d_p on the basis elements for every $p \in \{1, 2, ...\}$ as follows:

$$d_p : C_p(K) \to C_{p-1}(K), \quad \sigma \mapsto \sum_{\tau \subset \sigma, \tau \in K_{p-1}} \tau \tag{1}$$

and for $p = 0$, let d_0 be the zero map. Here and in the following, let K_p denote the set of all p-simplices. If the dimension of the simplicial complex K is n, then the set of p-simplices K_p is empty for all $p > n$. Hence, the corresponding vector space $C_p(K)$ is the zero vector space. As a consequence, the following sequence of vector spaces and $\mathbb{F}_2$-linear mappings is obtained:

$$0 \xrightarrow{d_{n+1}} C_n(K) \xrightarrow{d_n} \cdots \xrightarrow{d_2} C_1(K) \xrightarrow{d_1} C_0(K) \xrightarrow{d_0} 0, \tag{2}$$

which is also called a *chain complex*. The maps d_p are referred to as *boundary maps* and by simple calculations it follows that they have the property

$$d_p \circ d_{p+1} = 0 \text{ for all } p \in \{0, 1, 2, ...\}. \tag{3}$$

As a consequence, $\operatorname{im} d_{p+1} \subset \ker d_p$. This condition allows us to consider the quotient of the two vector spaces $\ker d_p$ and $\operatorname{im} d_{p+1}$.

Definition 3.3. For any $p \in \{0,1,2,...\}$, define $Z_p := \ker d_p$ and $B_p := \operatorname{im} d_{p+1}$. The elements of B_p are referred to as *p-boundaries* and the elements of Z_p are called *p-cycles*. Then, the quotient vector space

$$H_p(K) := Z_p / B_p \tag{4}$$

is called the *p-th homology* of a simplicial complex K. The *p-th Betti number* of the simplicial complex K is defined as the dimension of the p-th homology vector space,

$$\beta_p(K) := \dim H_p(K) = \dim Z_p - \dim B_p. \tag{5}$$

One property of homology is that maps between simplicial complexes $f : K \to L$ induce linear maps between the corresponding homology vector spaces $f_p : H_p(K) \to H_p(L)$ for all p. Another important property is *functoriality*: given maps of simplicial complexes $f : K \to L$ and $g : L \to M$, for the mapping $(g \circ f)_p : H_p(K) \to H_p(M)$ it holds that $(g \circ f)_p = g_p \circ f_p$.

3.3 Filtrations

A sequence of nested subcomplexes of a simplicial complex K

$$\emptyset = K_0 \subset K_1 \subset \cdots \subset K_l = K \tag{6}$$

is called a *filtration* of K. Considering the homology of each of the subcomplexes, for every $i \leq j$ the inclusion maps from K_i to K_j induce linear maps

$$f_p^{i,j} : H_p(K_i) \to H_p(K_j) \tag{7}$$

for all p. Consequently, we also obtain for each dimension p a sequence of homology spaces

$$0 = H_p(K_0) \to H_p(K_1) \to \cdots \to H_p(K_l) = H_p(K) \tag{8}$$

where the arrows between subsequent vector spaces $H_p(K_i)$ and $H_p(K_{i+1})$ are the above defined maps $f_p^{i,i+1}$. Due to the already mentioned functoriality condition it holds:

$$f_p^{j,k} \circ f_p^{i,j} = f_p^{i,k}, \qquad \text{for all } i \leq j \leq k. \tag{9}$$

Definition 3.4 (p-th persistent homology)**.** Consider a filtration of a simplicial complex $K_0 \subset K_1 \subset \cdots \subset K_l = K$. Then, the p-th persistent homology of K is defined as

$$H_p^{i,j} := \operatorname{im} f_p^{i,j} = Z_p(K_i) / (B_p(K_j) \cap Z_p(K_i)), \tag{10}$$

where $f_p^{i,j} : H_p(K_i) \to H_p(K_j)$ are the linear maps induced by the inclusions maps $K_i \to K_j$ for all i, j with $0 \leq i \leq j \leq l$.

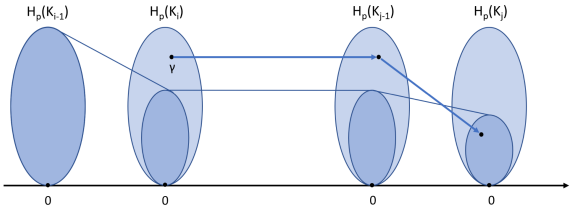

Figure 3: Class γ is born at filtration step i and dies entering filtration step j, inspired by (Edelsbrunner and Harer, 2010).

Definition 3.5. A homology class $\gamma \in H_p(K_i)$ is said to be *born* at filtration step i if $(f_p^{i-1,i})^{-1}(\gamma) = \emptyset$, i.e. it does not lie in the image of $f^{i-1,i}$. Intuitively, it means that i is the smallest index on which the class appears. Further, we say that a class $\gamma \in H_p(K_i)$ *dies* entering K_j if it merges with an older class as we go from K_{j-1} to K_j, that is, $f_p^{i,j-1}(\gamma) \notin H_p^{i-1,j-1}$ but $f_p^{i,j}(\gamma) \in H_p^{i-1,j}$. In the literature, this is referred to as *elder rule*.

The main idea of persistent homology is to track the *lifetime* of homology classes, i.e. when classes are born and when they die. Classes that *persist* on a large scale are regarded as actual features whereas classes with only a short lifetime are said to be caused by noise. A way to visualize this is through a set of intervals of the form $[b_i, d_i)$, where each interval corresponds to a class γ_i with birth time b_i and death time d_i. If a class with birth time b_j does not die throughout the entire filtration we say that it lives forever and associate it to the interval $[b_j, \infty)$. This collection of intervals is called the *barcode*.

Definition 3.6. A barcode is a finite set of half-open intervals $[i, j)$, where $0 \leq i < j \in \mathbb{R} \cup \{\infty\}$.

An equivalent way to visualize the lifetime of the persistent homology classes is the so-called *persistence diagram*, which is defined as a multiset of points in $\mathbb{R}^2$ where each class γ_i corresponds to a point (b_i, d_i). In Figure 5, Subfigures 5c and 5e, one can see an example for a barcode and a persistence diagram in dimensions 0 and 1, respectively. In a persistence diagram, points that are close to the diagonal correspond to short intervals and points far from the diagonal to long, persistent features. Since for every class it holds that it dies after it is born, i.e. $b_i < d_i$, all the points lie above the diagonal.

3.4 Comparison of Persistence Diagrams

For technical reasons, in the formal definition of a persistence diagram we also include each point on the diagonal $\Delta = \{(x,y) \in \mathbb{R}^2 | x = y\}$ with infinite multiplicity. This guarantees that there exists a bijection

for any two persistence diagrams by assuring that they have the same cardinality.

Definition 3.7 (Persistence diagram)**.** A persistence diagram is the union of a countable multiset of points (x,y) in $(\mathbb{R}\cup\{\infty\})^2$ with $x<y$ and the diagonal $\Delta=\{(x,y)\in\mathbb{R}^2|x=y\}$, where each point on the diagonal has infinite multiplicity. (Mileyko et al., 2011)

The most frequently used way to compare persistence diagrams or equivalently, barcodes, with each other is the bottleneck distance.

Definition 3.8 (Bottleneck distance)**.** The bottleneck distance between two persistence diagrams D_1 and D_2 is defined as

$$W_\infty(D_1,D_2)=\inf_{\varphi:D_1\to D_2}\sup_{x\in D_1}\|x-\varphi(x)\|_\infty, \quad (11)$$

where $\varphi:D_1\to D_2$ ranges over all bijections from D_1 to D_2. (Mileyko et al., 2011)

In words, the bottleneck distance is the longest distance of two matched points, where the matching between the two diagrams is chosen in an optimal way such that it minimizes the longest distance of two matched points. In Figure 4, one can see two persistence diagrams in red and blue, respectively, and the matching between the closest points. Points close to the diagonal are matched to the diagonal.

In the particular case where one computes the bottleneck distance of an arbitrary diagram D_1 and the empty diagram $D_\emptyset$ that contains only the diagonal, all the points in the first diagram are matched to the diagonal and the bottleneck distance is proportional to the length of the longest bar in the barcode.

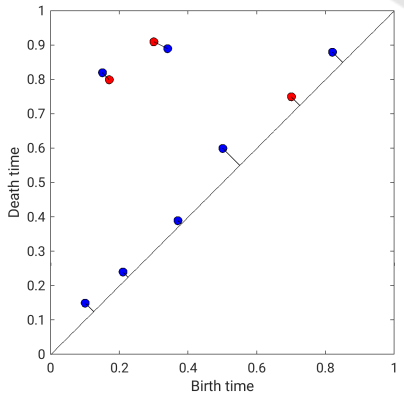

Figure 4: Example for the bottleneck distance for two persistence diagrams (red and blue).

4 EEG DATA

In order to apply DyCA to a multi-variate time series, a system of ordinary differential equations with both linear and non-linear equations has to be given to model the underlying dynamics. In (van Veen and Liley, 2006), the authors showed via bifurcation analysis the existence of Shilnikov chaos during epileptic seizures. The authors of (Friedrich and Uhl, 1996) verified that the dynamics in EEG data during epileptic seizures can be accurately modeled by the following system of differential equations

$$\begin{aligned}\dot{x}_1&=x_2,\\ \dot{x}_2&=x_3,\\ \dot{x}_3&=f(x_1,x_2,x_3),\end{aligned} \quad (12)$$

with f being a non-linear polynomial function. Hence, the assumptions for applying DyCA are fulfilled. However, if the patient is out of seizure, the system exhibits no structure.

For the experiments, we used EEG data from a German hospital that was measured with 25 channels using a sampling rate of 256 Hz. The data set consists of 6 time series with lengths of 10 to 40 seconds. The EEG was recorded from patients that suffer under a special kind of epilepsy with seizures that are called absence seizures or petit-mal seizures. These absences are characterized by impairment of consciousness and an abrupt beginning and end. Usually, absence seizures last from a few seconds to half a minute (Commission on Classification and Terminology of the International League Against Epilepsy, 1981).. We chose a moving window setup with windows of 0.5 second length in order to assure that the window size is long enough to contain at least one cycle of the recurrent trajectories and short enough to detect the absence. The beginning time of the moving window is shifted by 0.1s, resulting in an overlap of 80% for neighboring windows.

5 NUMERICAL EXPERIMENTS

5.1 Methodology

For the preprocessing with DyCA the algorithm as described in (Uhl et al., 2020) was used. All the computations of simplicial complexes, persistent homology and the bottleneck distance were performed by means of the software library JAVAPLEX (Tausz et al., 2014). Written in Java, it can be accessed from MATLAB and contents many relevant functions from persistent homology. It was applied to the point-cloud data that was obtained by applying DyCA on the entire multi-variate time series and windowing the resulting four dimensional data into windows of length 0.5 seconds. This resulted in approximately 128 points

in $\mathbb{R}^4$ per window. From this point-cloud data, a filtered Vietoris-Rips complex was calculated using the JAVAPLEX library. After applying persistent homology, the barcode for every window is calculated.

As mentioned in Section 4, during the epileptic seizures one assumes that there is structure in the data after projecting it with DyCA onto a lower-dimensional subspace. Contrarily, in time periods without epileptic seizures one assumes that the data has no structure. In order to distinguish these two states, our approach regards the 1-dimensional persistent homology of the windowed, projected time-series and compares the barcodes/persistent diagrams of every window with the empty diagram, i.e. the diagram which consists only of the diagonal. This is based on the assumption that in windows without an epileptic seizure there is no structure, hence in an ideal case there should be no persistent features. Thus, for every window the bottleneck distance is calculated between the persistence diagram of the current window and the empty diagram. For windows without an absence we expect the bottleneck distance to the empty diagram to be small whereas for windows where an epileptic event is happening we expect it to be higher.

In Figure 5, one can exemplary see the results for two windows, where Subfigures 5a, 5c and 5e were generated using a window during an epileptic event and Subfigures 5b, 5d and 5f correspond to a window without an absence. The length of the windows was chosen to be 0.7s in order to assure that the trajectory shows more than two cycles. In the actual experiments, a shorter window length is chosen to prevent the blurring of the transition time between the two states.

In the first row, the trajectory projected with DyCA is shown. To be precise, the point cloud was projected with DyCA onto a four dimensional subspace, but for sake of visibility only plots in a three dimensional subspace are shown.

In the second row, one can see the barcodes corresponding to the persistent homology of both windows in dimensions 0 and 1, respectively. The barcode during the absence shows a completely different behavior than the barcode in the window without an absence. In dimension 1, one can see that there are a lot of connected components during the absence until the filtration value, where all connected components merge to one component. A bit before all the connected components except for one die, the most persistent hole (feature in dimension 1) is born and it survives until filtration value 0.47. However, in 5c one can also see a lot of other non-persistent holes in dimension 1, but their lifetime is rather short. One could suspect that the second longest bar in the barcode of dimension 1 corresponds to the little hole in the trajectory, but it is hard to verify.

In Subfigures 5e and 5f, the corresponding persistence diagrams for both windows are shown. Red dots denote features in dimension 1 whereas blue dots correspond to features in dimension 0. The triangles denote features that do not die throughout the filtration and therefore they correspond to the arrows in the barcode of the 0-th persistent homology. As it was already mentioned, dots that are far from the diagonal correspond to long bars in the barcode. Hence, in Subfigure 5e the red dot that is far from the diagonal is the persistent hole and the dots near the diagonal are considered as topological noise. In case of the chaotic behavior, i.e. the trajectory in the window where no epileptic event is happening, there are no persistent holes visible. The only holes are three holes that are born right in the beginning of the filtration and die shortly after they are born. Hence, the multiplicity of the red dot in the persistence diagram in 5f is three. The barcode in dimension 0 in Subfigure 5d shows that there is only one connected component throughout the entire filtration. In order to differentiate windows with and without an epileptic event we consider the most persistent hole in dimension 1 as the distinction feature.

5.2 Results

In Figure 6, the results for the bottleneck distance obtained by applying the above described methodology to the 6 different EEG time series are shown. First of all, the given multi-variate time series is projected onto a 4 dimensional subspace using DyCA. Afterwards, at each time step the bottleneck distance of the persistence diagram of the point cloud in the corresponding window and the empty persistence diagram is calculated. Thus, the x-axis of every plot in Figure 6 shows the time in seconds and on the y-axis, one can see the bottleneck distance of the window starting at time x and ending at time $x + 0.5$s. The red dotted lines denote the beginning and the end of an absence, as it was detected by a medical doctor (expert). The beginning of an absence is marked with two dotted lines at a distance of 0.5s in order to indicate that the moment of the transition of the two state can only be determined with a precision subject to the window length. The second of the two lines that denote the beginning of an epileptic event is the starting time determined by the expert.

In Subfigures 6a, 6b, 6c and 6f, the beginning of the absence is detected sharply, whereas in Subfigures 6d and 6e the epileptic event seems to start shortly before the starting time that was detected by the expert.

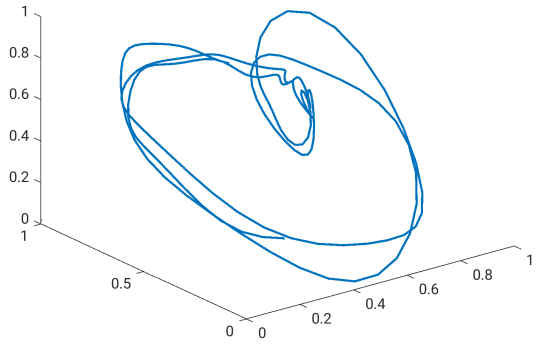

(a) Trajectory during absence.

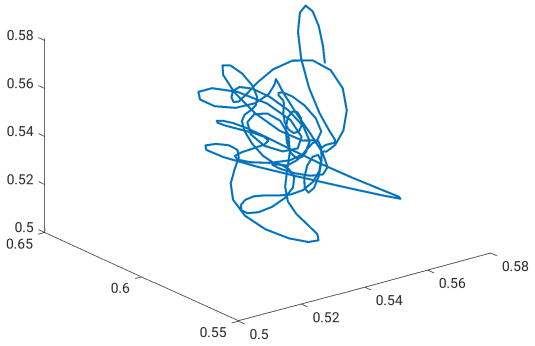

(b) Trajectory without absence.

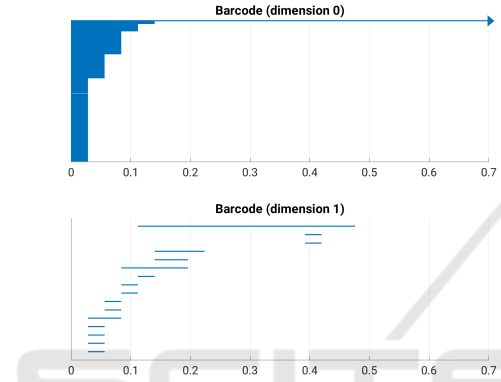

(c) Barcode during absence.

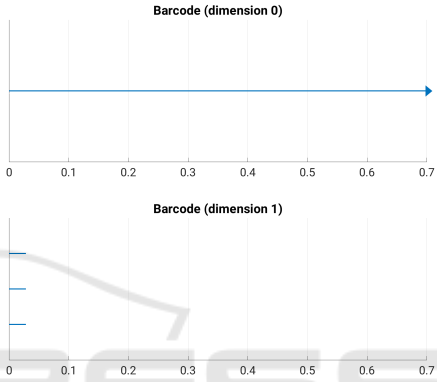

(d) Barcode without absence.

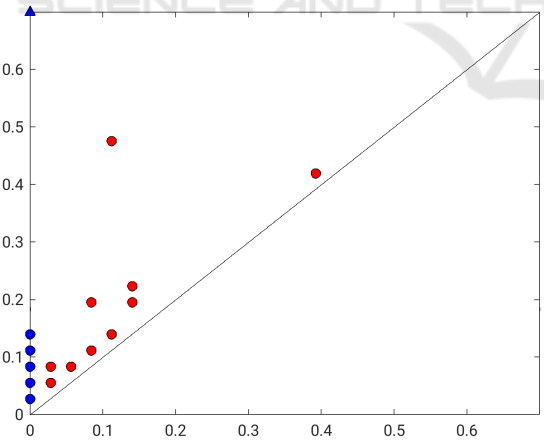

(e) Persistence diagram during absence.

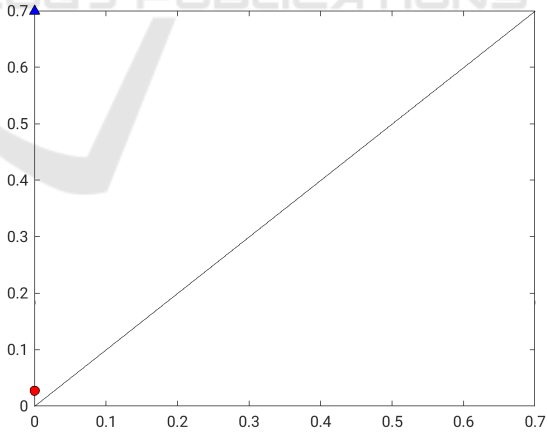

(f) Persistence diagram without absence.

Figure 5: Overview of the results for two exemplary windows with (left column) and without (right column) an epileptic seizure.

However, for each data set the end of an absence is sharp and is situated exactly where it was identified by the expert.

To get some numerical results, for every time series f_i we chose a threshold α_i, such that the classification task is performed in an optimal way. Windows where the bottleneck distance is above that threshold are classified as absence windows and windows with a lower bottleneck distance are categorized as windows without an epileptic event. In Table 1, one can see for

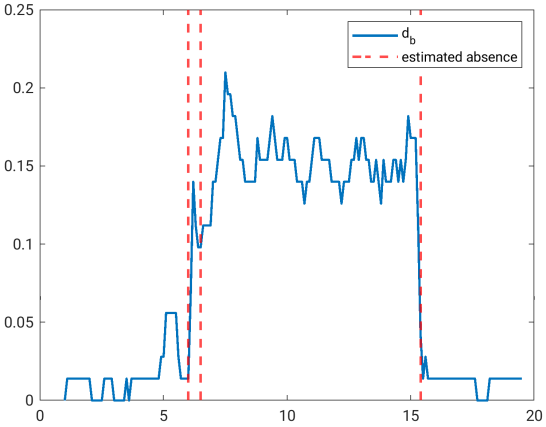

(a) Time Series 1.

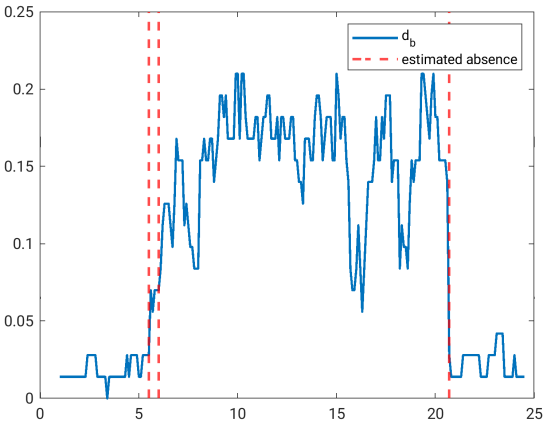

(b) Time Series 2.

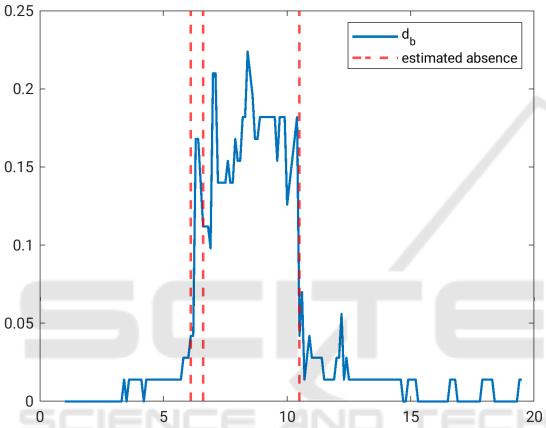

(c) Time Series 3.

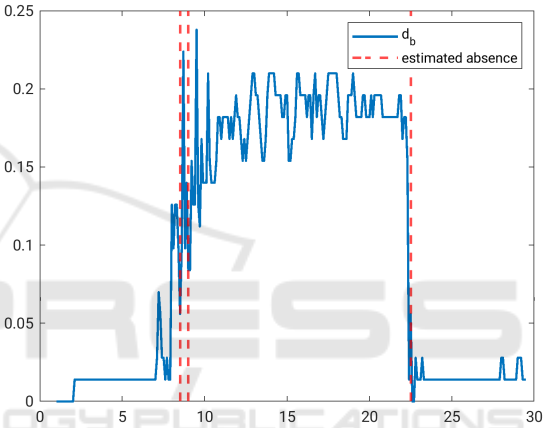

(d) Time Series 4.

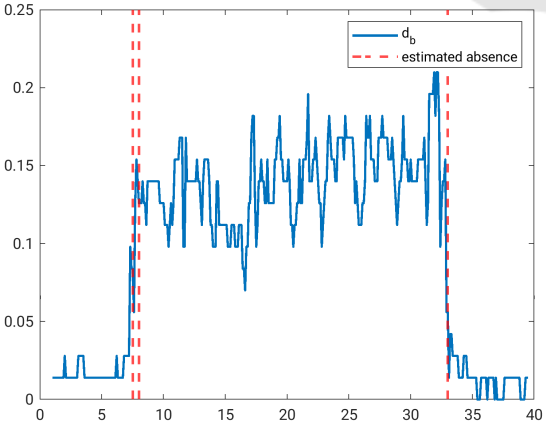

(e) Time Series 5.

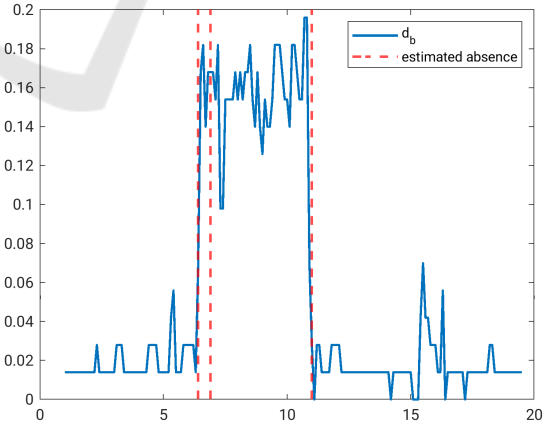

(f) Time Series 6.

Figure 6: Bottleneck distance d_B for 6 data sets to detect epileptic seizures.

every time series (TS) the chosen threshold value α and the resulting wrongly classified frames by using the threshold. In the last column, the corresponding percentage is shown. Since in Subfigures 6d and 6e the beginning of the absence is approximately half a second after the increase of the bottleneck distance, it is impossible to find a threshold α that divides the windows into windows with or without absence.

Table 1: Results for the classification task of the 6 evaluated data sets.

	α	Wrong frames	Percentage
TS 1	0.06	0/186	0%
TS 2	0.05	0/236	0%
TS 3	0.08	1/186	0.5%
TS 4	0.08	6/286	2.1%
TS 5	0.05	4/386	1.0%
TS 6	0.08	1/186	0.5%

Even though there are some outliers, such as in Subfigure 6f around second 15.6 and in Subfigure 6b around second 16.3, the results show a clear difference between windows in which an epileptic event occurs and windows without an epileptic event. Furthermore, the results in Table 1 show that we achieve a very good classification performance with our proposed approach, with the percentage of falsely categorized frames ranging from 0% to 2.1%. Additionally, it shows that without an epileptic event the conditions of the DyCA are not fulfilled and hence it fails. We conclude that the combination of DyCA and persistent homology is well-suited to detect absence seizures in EEG data.

6 OUTLOOK

Despite the promising results presented in the previous Section, there are still some improvements that can be done. To be precise, EEG data can vary a lot between different patients as well as between different hospitals and measurement setups. Hence, the structure of the projected trajectory with DyCA can differ a lot, making the relevant holes more or less persistent. Also, adding a data point that lies exactly in the center of the most persistent cycle considerably alters the persistence diagram. Hence, even though persistent homology is robust with respect to small perturbation of the input data, it is not very robust with respect to single outliers, that lie significantly outside the structure. Future work could address this issue, either by making the DyCA more robust or by using some sophisticated extensions of persistent homology.

Additionally, the structure of the attractor resembles more than one loop, i.e. an outer big loop and a smaller loop inside. However, in our investigation we only assumed that there is one relevant hole whose persistence was used as a classification feature. As an improvement, one could use more advanced techniques that include the information of the entire persistence diagram.

As last point, we would like to mention that the authors of this paper are aware of two other papers, (Piangerelli et al., 2018) and (Merelli et al., 2016), that also investigate the use of persistent homology to detect the differences between the states where epileptic events occur (ictal states) and the states without event or right before the event (preictal state), respectively. To discriminate the respective states they used an entropy measure that can be defined on barcodes, called the persistent entropy. By calculating a Pearson correlation coefficient matrix between windows of the time series and using it as weighted edges, that give rise to a filtration of a simplicial complex, and computing the persistent entropy of every barcode, the authors of (Merelli et al., 2016) showed that when it comes to the phase transition between the preictal and the ictal state the number of connected components drops to one and increases again after the phase transition. Additionally, in (Piangerelli et al., 2018) the authors discriminated epileptic states from non-epileptic ones by regarding each channel as a piecewise linear function, from which a so-called lower-star filtration of a simplicial complex can be computed. From each filtered simplicial complex they calculated the persistent entropy and averaged this value over all channels, using the result to train a supervised classifier. They got a strong separation of the values for the averaged persistence entropy between the two states. However, the comparison of our approach to the approaches mentioned above is out of the scope of this paper and will be addressed in subsequent papers, this is ongoing research.

ACKNOWLEDGEMENTS

This work has been supported by the German Federal Ministry of Education and Research (BMBF-Projekt 05M20WWA: Verbundprojekt 05M2020 - DyCA).

REFERENCES

Commission on Classification and Terminology of the International League Against Epilepsy (1981). Proposal for revised clinical and electroencephalographic classification of epileptic seizures. *Epilepsia*, 22(4):489–501.

Edelsbrunner, H. and Harer, J. (2010). *Computational Topology: An Introduction*. Applied Mathematics. American Mathematical Society, Providence, RI.

Friedrich, R. and Uhl, C. (1996). Spatio-temporal analysis of human electroencephalograms: Petit-mal epilepsy. *Physica D: Nonlinear Phenomena*, 98(1):171–182.

Merelli, E., Piangerelli, M., Rucco, M., and Toller, D. (2016). A topological approach for multivariate time series characterization: The epileptic brain. In

Proceedings of the 9th EAI International Conference on Bio-Inspired Information and Communications Technologies (Formerly BIONETICS), BICT'15, page 201–204, Brussels, BEL. ICST (Institute for Computer Sciences, Social-Informatics and Telecommunications Engineering).

Mileyko, Y., Mukherjee, S., and Harer, J. (2011). Probability measures on the space of persistence diagrams. *Inverse Problems*, 27(12):124007.

Otter, N., Porter, M. A., Tillmann, U., Grindrod, P., and Harrington, H. A. (2017). A roadmap for the computation of persistent homology. *EPJ Data Science*, 6(17).

Piangerelli, M., Rucco, M., Tesei, L., and Merelli, E. (2018). Topological classifier for detecting the emergence of epileptic seizures. *BMC Research Notes*, 11(1).

Tausz, A., Vejdemo-Johansson, M., and Adams, H. (2014). *JavaPlex: A research software package for persistent (co)homology*, pages 129–136. Lecture Notes in Computer Science 8592. Springer, Berlin.

Uhl, C., Kern, M., Warmuth, M., and Seifert, B. (2020). Subspace detection and blind source separation of multivariate signals by dynamical component analysis (dyca). *IEEE Open Journal of Signal Processing*, 1:230–241.

van Veen, L. and Liley, D. T. J. (2006). Chaos via Shilnikov's saddle-node bifurcation in a theory of the electroencephalogram. *Phys. Rev. Lett.*, 97:208101.